Orthotropic elastic constants of a boronaluminum fiberreinforced composite: An acousticresonancespectroscopy study

Hassel Ledbetter, Christopher Fortunko, and Paul Heyliger

Citation: Journal of Applied Physics **78**, 1542 (1995); doi: 10.1063/1.360247
View online: http://dx.doi.org/10.1063/1.360247
View Table of Contents: http://scitation.aip.org/content/aip/journal/jap/78/3?ver=pdfcov
Published by the AIP Publishing

Orthotropic elastic constants of a boron-aluminum fiber-reinforced composite: An acoustic-resonance-spectroscopy study

Hassel Ledbetter and Christopher Fortunko
Materials Science and Engineering Laboratory, National Institute of Standards and Technology, Boulder, Colorado 80303

Paul Heyliger
Civil Engineering Department, Colorado State University, Fort Collins, Colorado 80523

(Received 4 April 1994; accepted for publication 7 April 1995)

Acoustic-resonance spectroscopy was used to determine the complete elastic constants of a uniaxial-fiber-reinforced metal-matrix composite: boron-aluminum. This material exhibits orthotropic macroscopic symmetry and, therefore, nine independent elastic stiffnesses C_{ij}. The off-diagonal elastic constants (C_{12},C_{13},C_{23}), which contain large errors when measured by conventional methods, were especially focused on. Good agreement emerged among present results, a previous pulse-echo study, and theoretical predictions using a plane-scattered-wave ensemble-average model. Attempts to measure the internal-friction "tensor" failed. © *1995 American Institute of Physics.*

I. INTRODUCTION

Previous attempts to measure the elastic constants of fiber-reinforced orthotropic-symmetry composites suffer from various deficiencies. In a rod-resonance approach,[1] insufficiently thick plates preclude a complete C_{ij} determination because it is difficult to prepare out-of-plane rod-shape specimens. Also, this approach requires at least nine rod-shape specimens. For orthotropic symmetry, a pulse-echo approach[2] requires four specimens oriented differently with respect to principal axes. Using these one can measure 18 sound velocities, which overdetermine the nine C_{ij}.

Both approaches suffer from large error propagation for the off-diagonal elastic constants. To get S_{12}, for example, from rod-resonance measurements, we use a relationship such as the following:

$$S_{12}=\frac{S'_{11}-a_{11}^4S_{11}-a_{12}^4S_{22}-a_{11}^2a_{12}^2S_{66}}{2a_{11}^2a_{12}^2}. \tag{1}$$

Here x_1, x_2, x_3 are principal symmetry axes, a_{ij} denote direction cosines between primed (rotated) and nonprimed (natural) axes, and S'_{11} denotes reciprocal Young modulus in an arbitrary direction, but usually within a principal plane; in Eq. (1), within the x_1-x_2 plane. If the specimen is oriented perfectly (no a_{ij} errors), the uncertainty in S_{12} depends on uncertainties in S'_{11}, S_{11}, S_{22}, S_{66}.

For the pulse-echo case, error propagation is potentially worse. A typical expression for an off-diagonal elastic stiffness is the following:

$$C_{12}=\pm\{[2\rho v^2-\tfrac{1}{2}(C_{11}+C_{22}+2C_{66})]^2 - \tfrac{1}{4}(C_{22}-C_{11})^2\}^{1/2}-C_{66}. \tag{2}$$

Here ρv^2 denotes the product of mass density and squared sound velocity measured in a [110] direction. Thus, the uncertainty in C_{12} depends on uncertainties in ρv^2, C_{11}, C_{22}, C_{66}.

The off-diagonal C_{ij} (S_{ij}) are important for many reasons. Without them we cannot determine a material's most basic elastic constant, the bulk modulus (or reciprocal compressibility),

$$B=(C_{11}+C_{22}+C_{33}+2C_{12}+2C_{13}+2C_{23})/9, \tag{3}$$

we cannot know a material's Poisson ratios,

$$\upsilon_{ij}=-S_{ij}/S_{ii}, \tag{4}$$

and we cannot calculate through Hooke's law the strains arising from a simple stress,

$$\epsilon_{ij}=\sum_{k,l} S_{ijkl}\sigma_{kl}. \tag{5}$$

Acoustic-resonance spectroscopy avoids these error-propagation problems by using a single simple-geometry

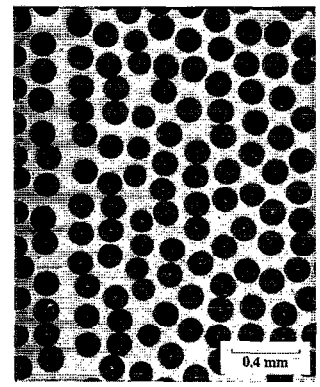

FIG. 1. Photomicrograph showing transverse-plane distribution of boron fibers in an aluminum matrix. Fiber volume fraction equals 48 vol %. Coordinate axes: x_3 perpendicular to page, x_1 horizontal, x_2 vertical. Nonuniform fiber distribution and other imperfections interfere with the acoustic-resonance-spectroscopy measurement method and, indeed, with all measurement methods.

 0021-8979/95/78(3)/1542/5/$6.00

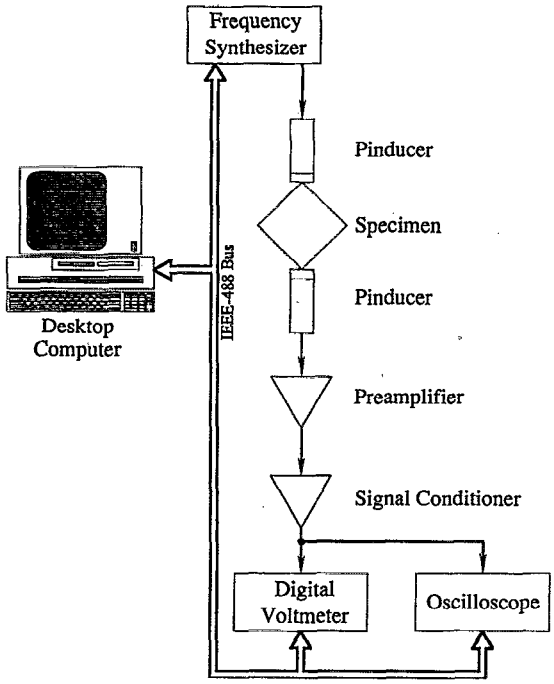

FIG. 2. Block diagram of measurement facility. The oscilloscope is optional.

specimen. All nine C_{ij} (or S_{ij}) result from analyzing a specimen's macroscopic vibrational frequencies. Thus, C_{12}, C_{13}, C_{23} are found on the same footing as the six diagonal C_{ij}, the C_{ii}.

II. MEASUREMENTS

A. Material

The studied composite had 0.14-mm-diam uniaxial boron fibers in a matrix of 6061 aluminum alloy. The aluminum alloy was in the F-tempered condition (as diffusion bonded). The composite, containing 48 vol % fibers, was fabricated as a plate measuring about $10\times10\times1.1$ cm^3. It was fabricated commercially according to the authors' specifications to provide sufficient material for elastic-constant studies. Figure 1 shows the microstructure. We chose x_3 as the filament axis, x_1 as the plate normal, and x_2 as the third orthogonal direction. Measured by Archimedes's method, we found the mass density $\rho=2.534$ g/cm^3. The specimen consisted of a $0.49\times1.12\times1.45$ cm^3 rectangular parallelepiped with a mass of 2.01 g.

B. Method

Figure 2 shows a block diagram of the apparatus used to measure the mechanical-resonance characteristics of the boron-aluminum specimens. The apparatus currently contains commercially available pinducers to generate and detect the specimen's mechanical vibrations.[3] The useful frequency range of the transducers extends from approximately 60 kHz to 1.5 MHz. In this frequency region, the pinducer's output voltage is generally proportional to the mechanical displacement at the surface of the specimen. The specimen is typically held between two coaxially aligned pinducers, which are spring loaded.

The mechanical-resonance measurements are typically carried out as follows. A stable, computer-controlled oscillator (frequency synthesizer) is used to drive one of the pin-

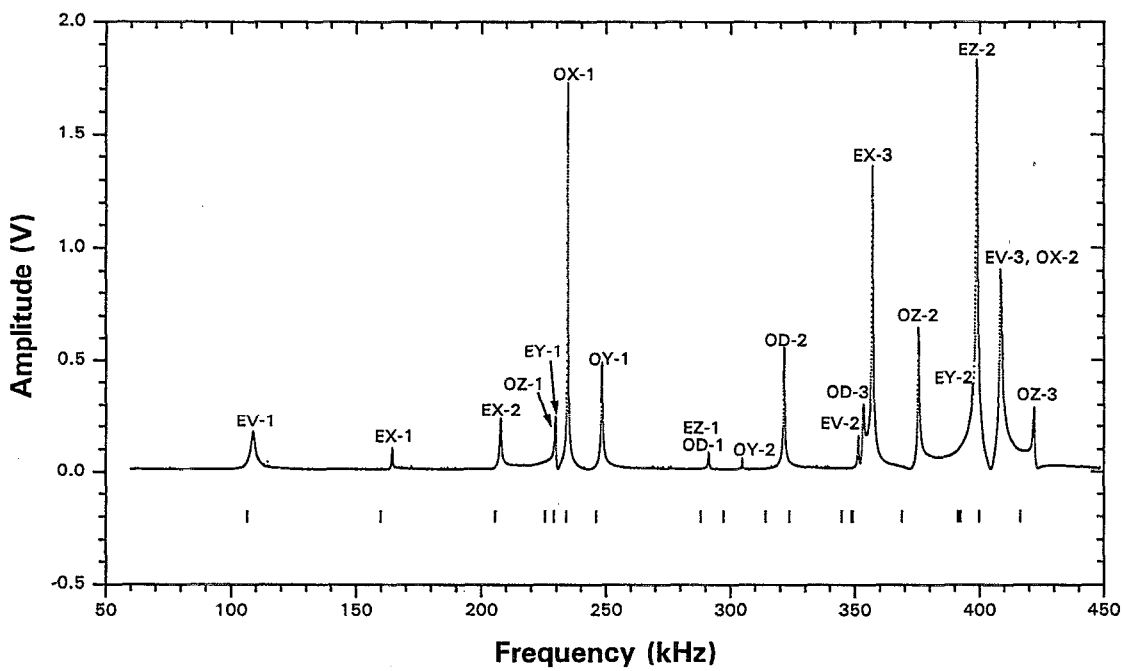

FIG. 3. Spectrum of resonance peaks. Through an inversion procedure, resonance frequencies lead to elastic stiffnesses C_{ij}. Driving amplitude equals 3.5 V. Bars at the bottom indicate predicted frequencies. Peak labeling follows the method established by Ohno (Ref. 5).

ducers with a sine-wave signal at approximately 10-V peak amplitude. The second pinducer is then used as the detector. The output of the detector pinducer is first preamplified by a high-impedance, low-noise amplifier with 10 MHz bandwidth. The signal is then processed with a signal conditioner, which acts as an amplifier with 20 or 40 dB gain and low-pass filter with 2 MHz corner frequency.

Finally, the amplitude of the output signal is measured directly with a high-quality digital voltmeter along with a digital oscilloscope. The frequency of the stable oscillator can be set within ± 1 Hz with 0.1 mHz resolution. The signal-to-noise performance of the apparatus shown in Fig. 2 usually exceeds 60 dB. Consequently, high-accuracy measurements of the resonance-peak amplitude characteristics can be made. Figure 3 shows the amplitude-frequency response. By measuring the elastic constants of a standard material, monocrystal copper, we estimate the C_{ij} measurement uncertainty as less than 0.5% and probably near 0.1%.

III. NUMERICAL MODEL

A. Variational statement

The numerical model uses a conventional application of the Ritz method by seeking approximate solutions to the weak form of the equations of motion for a parallelepiped under periodic vibration. The weak form of the equations of motion can be obtained by using a direct application of Hamilton's principle. This is effectively a dynamic statement of the principle of virtual work; it can be written as follows:

$$0=-\int_0^t\int_V \sigma_1\delta\epsilon_1+\sigma_2\delta\epsilon_2+\sigma_3\delta\epsilon_3+\sigma_4\delta\epsilon_4+\sigma_5\delta\epsilon_5 + \sigma_6\delta\epsilon_6\, dV\, dt+\tfrac{1}{2}\delta\int_0^t\int_V \rho(\dot{u}_1^2+\dot{u}_2^2+\dot{u}_3^2)dV\, dt. \tag{6}$$

Here V denotes the volume of the solid, $\dot{u}=\partial u/\partial t$, t is time, ρ the material density, δ the variational operator, u_1, u_2, and u_3 the dependent unknowns that represent the displacement components in the three coordinate directions that can undergo arbitrary variations, σ_i and ϵ_i denote components of stress and strain, and the conventional contracted notation ($\sigma_1=\sigma_{11}$, $\sigma_4=\sigma_{23}$, and so on) has been used. For the free-vibration problem there are no applied external loads, and each face of the solid is assumed stress free. Hence, in the statement of Hamilton's principle there are no nonzero surface terms involving specified displacements or tractions.

The displacements can be expressed as $u_1=U(x,y,z)$, $u_2=V(x,y,z)$, and $u_3=W(x,y,z)$. The strain-displacement relations are given by

$$\epsilon_{11}=\frac{\partial U}{\partial x},\quad \epsilon_{22}=\frac{\partial V}{\partial y},\quad \epsilon_{33}=\frac{\partial W}{\partial z},$$
$$\gamma_{12}=\frac{\partial V}{\partial x}+\frac{\partial U}{\partial y},\quad \gamma_{13}=\frac{\partial U}{\partial z}+\frac{\partial W}{\partial x},\quad \gamma_{23}=\frac{\partial V}{\partial z}+\frac{\partial W}{\partial y}. \tag{7}$$

Substitution of these equations and the stress-strain relations into Eq. (6) gives the weak form as

$$\delta U=\int_V\Bigg[\left(C_{11}\frac{\partial U}{\partial x}+C_{12}\frac{\partial V}{\partial y}+C_{13}\frac{\partial W}{\partial z}\right)\frac{\partial\delta U}{\partial x}+\left(C_{12}\frac{\partial U}{\partial x}+C_{22}\frac{\partial V}{\partial y}+C_{23}\frac{\partial W}{\partial z}\right)\frac{\partial\delta V}{\partial y}+\left(C_{13}\frac{\partial U}{\partial x}+C_{23}\frac{\partial V}{\partial y}+C_{33}\frac{\partial W}{\partial z}\right)\frac{\partial\delta W}{\partial z}+C_{44}\left(\frac{\partial V}{\partial z}+\frac{\partial W}{\partial y}\right)\left(\frac{\partial\delta U}{\partial y}+\frac{\partial\delta W}{\partial y}\right)+C_{55}\left(\frac{\partial U}{\partial z}+\frac{\partial W}{\partial x}\right)\left(\frac{\partial\delta U}{\partial z}+\frac{\partial\delta W}{\partial x}\right)+C_{66}\left(\frac{\partial U}{\partial y}+\frac{\partial V}{\partial x}\right)\left(\frac{\partial\delta U}{\partial y}+\frac{\partial\delta V}{\partial x}\right)-\rho\omega^2(U\delta U+V\delta V+W\delta W)\Bigg]dV. \tag{8}$$

B. Ritz approximations

The Ritz method seeks approximate solutions to the weak form given in Eq. (8). This is accomplished by approximating the displacement components U, V, W using finite linear combinations of the form

$$U(x_1,x_2,x_3)=\phi_0^U(x_1,x_2,x_3)+\sum_{j=1}^{n} a_j\phi_j^U(x_1,x_2,x_3),$$
$$V(x_1,x_2,x_3)=\phi_0^V(x_1,x_2,x_3)+\sum_{j=1}^{n} b_j\phi_j^V(x_1,x_2,x_3), \tag{9}$$
$$W(x_1,x_2,x_3)=\phi_0^W(x_1,x_2,x_3)+\sum_{j=1}^{n} d_j\phi_j^W(x_1,x_2,x_3).$$

Here ϕ_j^U and so on are known functions of position, n represents the number of terms in the approximation for the displacement components, and a_j, b_j, d_j are constants determined by requiring that each of the variational statements holds for arbitrary variations of U, V, W. This requirement is equivalent to the weak forms holding for arbitrary variations of a_j, b_j, d_j. In this study, power series in the coordinate variables x, y, z are used to approximate the displacements. Substitution of the approximate displacements and their variations into the weak form results in a matrix equation whose solution can be obtained from any standard eigenvalue routine.

C. Inverse procedure

The frequencies predicted using the approximate solutions by theory of elasticity are used with the measured fre-

TABLE I. Elastic-stiffness constants of a 48 vol % boron-aluminum fiber-reinforced composite, in units of GPa.

C_{ij}	Resonance[a]	Pulse echo[b]	Acoustic-resonance spectroscopy	Theory[c]
11	189.6±3.8	185.2±0.9	185.9±1.9	179.0
22	189.6±3.8	179.7±0.9	183.5±1.8	179.0
33	246.4±4.9	245.0±1.2	246.1±2.5	256.0
44	57.0±0.6	56.6±0.6	55.1±0.6	55.9
55	57.0±0.6	56.9±0.6	55.8±0.6	55.9
66	47.1±0.5	52.6±0.6	50.8±0.5	52.3
12	95±24	77.9±1.6	74.9±0.7	74.5
13	48±12	60.6±1.2	60.3±0.6	58.3
23	48±12	60.4±1.2	59.4±0.6	58.3

[a]Derived by inverting the S_{ij} matrix in Ref. 1, which contains an imposed artificial transverse-isotropic (five-constant) symmetry.
[b]Reference 2.
[c]Reference 4. Imposed artificial transverse-isotropic symmetry.

quencies to compute an optimal set of elastic constants. In general, an error function is formed equal to the square root of the sum of the squares of the differences (or the differences themselves) between the first n frequencies. The minimum of this function is then sought using some minimization routine. In the present study, the lowest 20 measured frequencies were used. The conjugate gradient method was used to minimize the error function using nine unknowns: the C_{ij}.

Initial estimates are required for the unknown elastic constants. These were provided by previous pulse-echo measurements. The minimization routine was allowed to iterate until there was no change in the sixth significant figure for the dependent unknowns.

IV. RESULTS

Table I shows the acoustic-resonance-spectroscopy results together with those from rod-resonance[1] and pulse-echo[2] measurements. Also included are theoretical predictions from a scattered-plane-wave ensemble-average model.[4] As input, the theory requires only the two constituents' elastic constants and the fiber volume fraction.

V. DISCUSSION

Our results show, for the first time we think, that acoustic-resonance spectroscopy applies to a two-phase fiber-reinforced material. The specimen shows natural macroscopic vibration frequencies like those obtained for an anisotropic monophase material. In the first 20 resonance peaks, no spurious peaks appeared and no expected peaks were missing.

This material's orthorhombicity is small but real and shows about equally in $C_{22}\neq C_{11}$, $C_{55}\neq C_{44}$, and $C_{23}\neq C_{13}$: longitudinal, shear, and off-diagonal elastic stiffnesses. It shows slightly more strongly in $C_{66}\neq (C_{11}-C_{12})/2$. We attribute the material's orthorhombicity to its manufacture: to the use of layups and uniaxial stress perpendicular to the plate.

Comparing spectroscopy results with theory—especially for C_{11}, C_{22}, C_{33}—suggests that the fibers contain a texture that makes them slightly anisotropic: The stiffness is higher perpendicular to the fiber and lower along the fiber compared with that of isotropic boron.

The off-diagonal C_{ij} (C_{12}, C_{13}, C_{33}) now seem to be known within a few percent, perhaps the best we can expect for a composite material where various internal defects must occur. These defects include nonhomogeneous fiber distribution, nonparallel fibers, and fiber misorientations with respect to principal axes.

From the microstructure, we can make some predictions about relative elastic constants without using theoretical models. First, because the fibers are stiffer than the matrix and lie along [001], we expect $C_{33}>C_{11}\simeq C_{22}$. Second, because the material processing involved compressive stress along [100], the fiber density along [100] slightly exceeds that along [010]; thus, $C_{11}>C_{22}$, slightly. For the shear moduli, we expect $C_{44}\simeq C_{55}>C_{66}$ because $C_{66}=C_{1212}$; the shear of the x_1 plane in the x_2 direction (or vice versa) involves mainly matrix shear without changing fiber arrangement. The $C_{44}-C_{55}$ relative magnitude is difficult to predict.

Turning to the off-diagonal elastic constants, it is simpler to reason about the S_{ij} using the inverse Hooke's law,

$$\epsilon_{ij}=S_{ijkl}\sigma_{kl}. \tag{10}$$

This leads to quite simple gedanken experiments where we apply a simple uniaxial stress along a principal axis and reason about the strain responses ϵ_{11}, ϵ_{22}, ϵ_{33} from the relative stiffnesses $C_{33}>C_{11}>C_{22}$ or relative compliances $S_{22}>S_{11}>S_{33}$. Consider first a stress along x_1. It follows that

$$\frac{\epsilon_2}{\epsilon_3}=\frac{S_{21}\sigma_1}{S_{31}\sigma_1}=\frac{S_{12}}{S_{13}}. \tag{11}$$

Because $\epsilon_2>\epsilon_3$ (fibers are stiffer) it follows that

$$|S_{12}|>|S_{13}|. \tag{12}$$

For this material, and most others, all the off-diagonal S_{ij} are negative. Similar reasoning for a stress along x_2 gives

$$|S_{12}|>|S_{23}|. \tag{13}$$

Finally, reasoning for a stress along x_3 gives

$$|S_{23}|>|S_{13}|. \tag{14}$$

If we invert the C_{ij} matrix to get the S_{ij} matrix, we find that all three relationships, Eqs. (12)–(14), hold for the boron-aluminum material, that is, $|S_{12}|>|S_{23}|>|S_{13}|$, the numbers being -2.4, -1.1, -1.0 TPa^{-1}.

Finally, we mention our attempt to determine the material's internal friction C_{ij}^*, the imaginary part of the total elastic constant,

$$\tilde{C}_{ij}=C_{ij}+iC_{ij}^*. \tag{15}$$

Similarly to inverting the vibration frequencies f_i to get the C_{ij}, we can invert the widths of the resonance peaks $\Delta f_i/f_i$ to get the C_{ij}^*. This attempt failed: The results were nonphysical, some impossibly negative. We think that this attempt failed because no single internal-friction mechanism (related strongly to the principal axes) dominates in this material. In some systems, such a dominant internal-friction source should occur. For example, in copper monocrystals

we believe that internal friction arises principally from dislocations vibrating in certain crystallographic planes and directions. In composites such as that in the present study, internal friction may arise from many different sources, thus defying simple analysis. For example, imagine two sources: dislocations in the matrix and fiber-matrix-interface separation. If the matrix were a random polycrystal, then all macroscopic C_{ij}^* would be affected more or less equally. Interface separation (without sliding) would affect only C_{11}^* and C_{22}^*. Thus, in these complicated materials, internal-friction measurement needs to combine acoustic-resonance spectroscopy with methods that excite a single deformation mode, for example, torsion or bending.

VI. CONCLUSIONS

(1) Acoustic-resonance spectroscopy works for two-phase fiber-reinforced materials.
(2) Considering all nine C_{ij}, the spectroscopy results agree, on average, within 2% with previous pulse-echo results. Agreement is best (1%) for the longitudinal C_{ij} and worst (3%) for the transverse C_{ii}.
(3) Surprisingly, the average off-diagonal C_{ij} spectroscopy/pulse-echo disagreement is only 2%.
(4) Among the measurement methods considered here, acoustic-resonance spectroscopy is preferred. It requires a single simple specimen, no transducer-specimen couplant, and works for quite small specimens. For measuring temperature or pressure effects, the spectroscopy method offers obvious advantages: one run instead of nine or more.
(5) This material contains too many complexities for the companion analysis of the internal friction C_{ij}^*.
(6) Measurements confirm several simple elastic-constant interrelationships deduced from the microstructure.

ACKNOWLEDGMENT

Gratefully, we acknowledge Sudook Kim's help with measurements, without which this study would not have proceeded.

[1] D. Read and H. Ledbetter, J. Appl. Phys. **48**, 2827 (1977).
[2] H. Ledbetter, J. Appl. Phys. **50**, 8247 (1979).
[3] C. Fortunko, M. Hamstad, and D. Fitting, in *Proceedings of the 1992 Ultrasonics Symposium*, edited by B. McAvoy (IEEE, New York, 1992), p. 327.
[4] S. Datta and H. Ledbetter, Int. J. Solids Structures **19**, 885 (1983).
[5] I. Ohno, J. Phys. Earth **24**, 355 (1976).